Fifty years long soil development due to seasonal water-saturation under hydric conditions

Zoltán SZALAI, Marianna RINGER, Péter SIPOS, Tibor NÉMETH, Péter PEKKER and Gergely JAKAB

szalai.zoltán@csfk.org

Geographical Institute, Research Centre for Astronomy and Earth Sciences , Hungary
www.csfk.org

timeframe of the pedogenesis

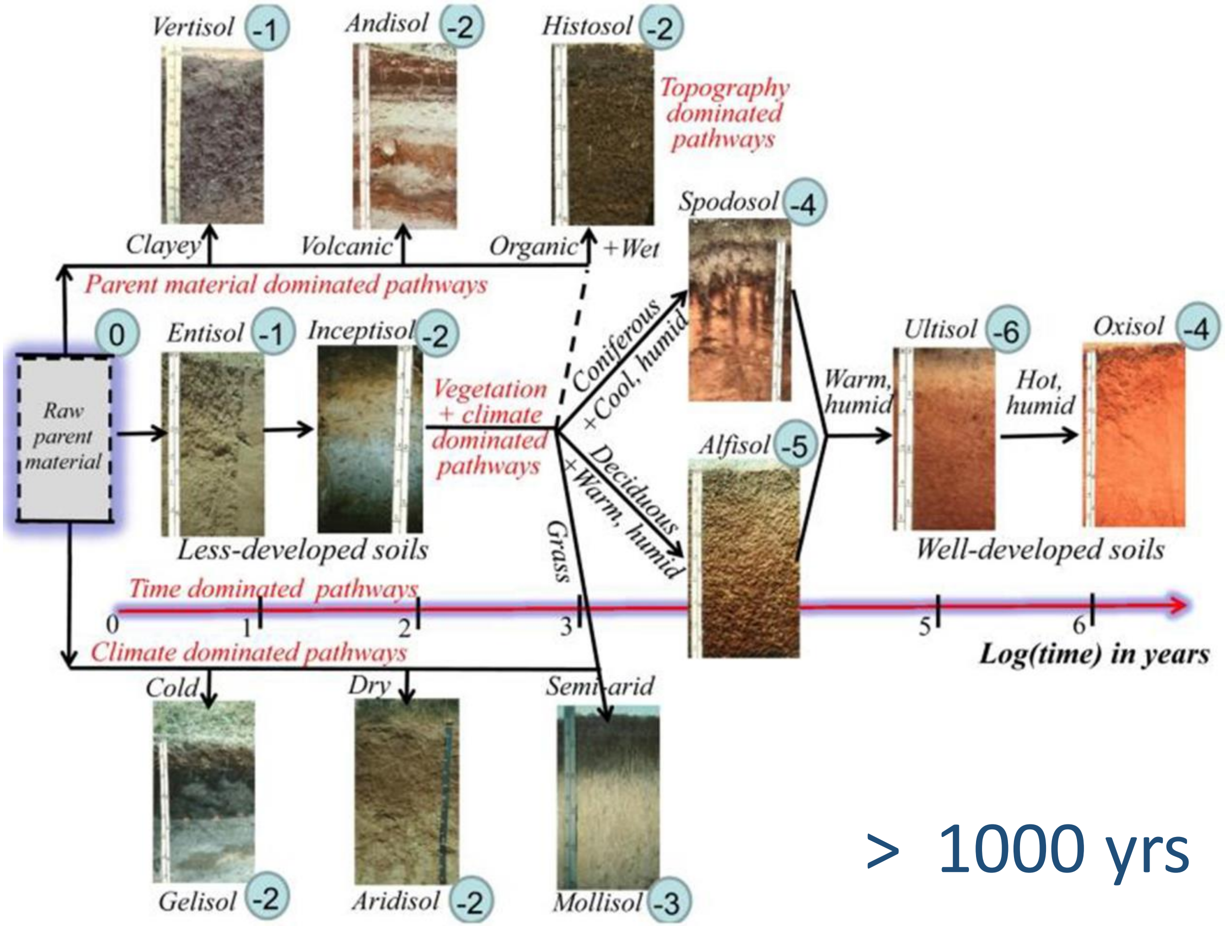

> 1000 yrs

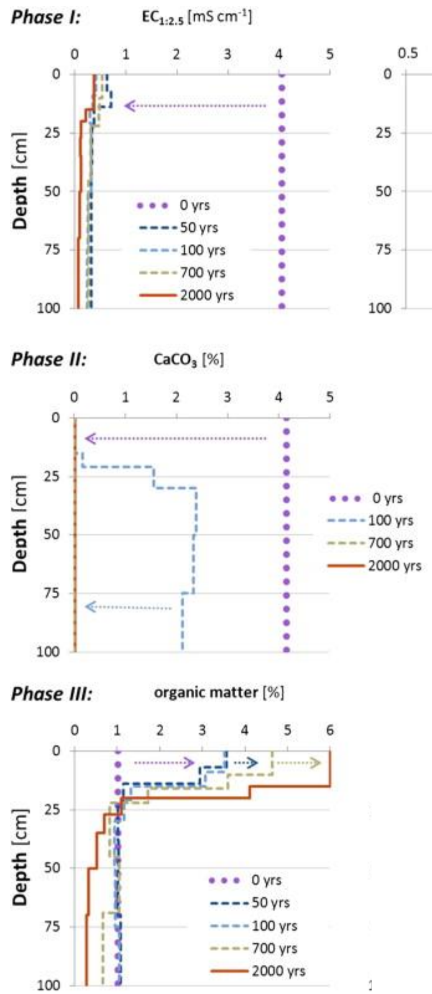

> 500 yrs

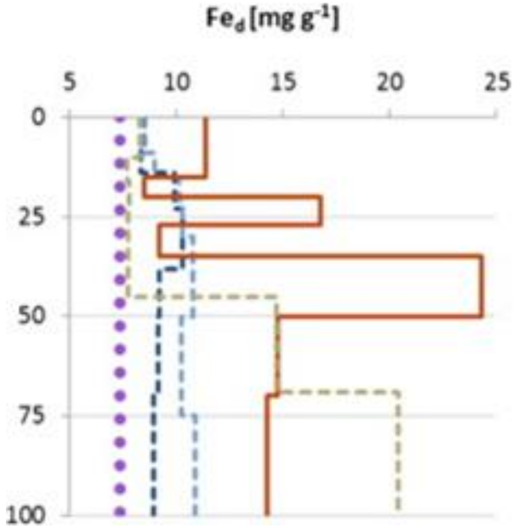

H. LIN, SSSAJ, 2011.
https://doi.org/10.2136/sssaj2011.0130
Three Principles of Soil Change and Pedogenesis in Space and Time

A KÖBL et al. GEODERMA, 2013.
https://doi.org/10.1016/j.geoderma.2013.09.005
Accelerated soil formation due to paddy management on marshland

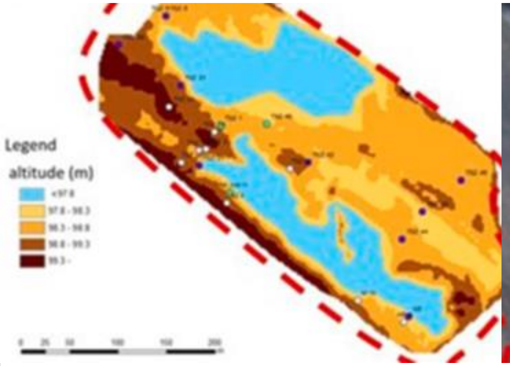

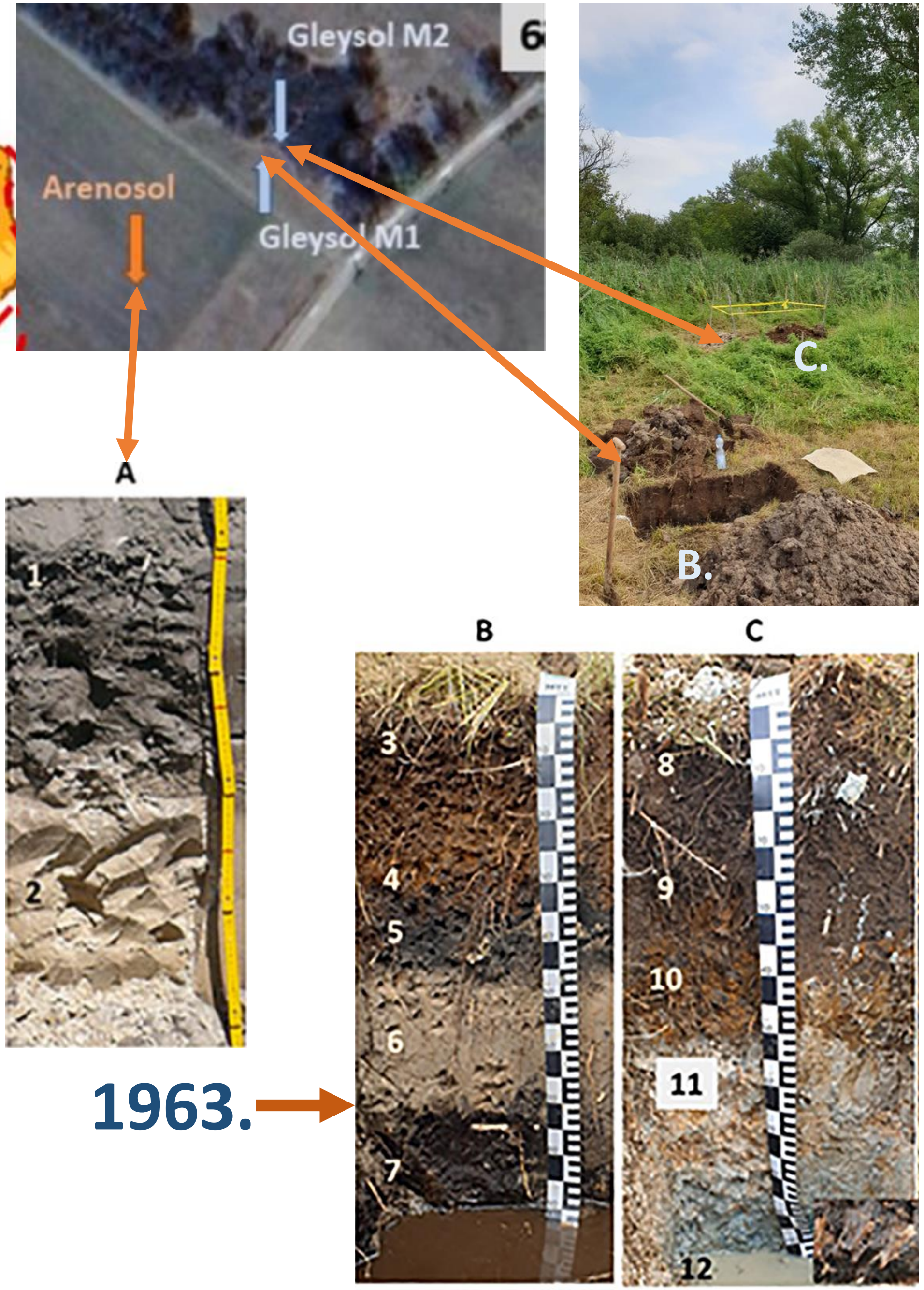

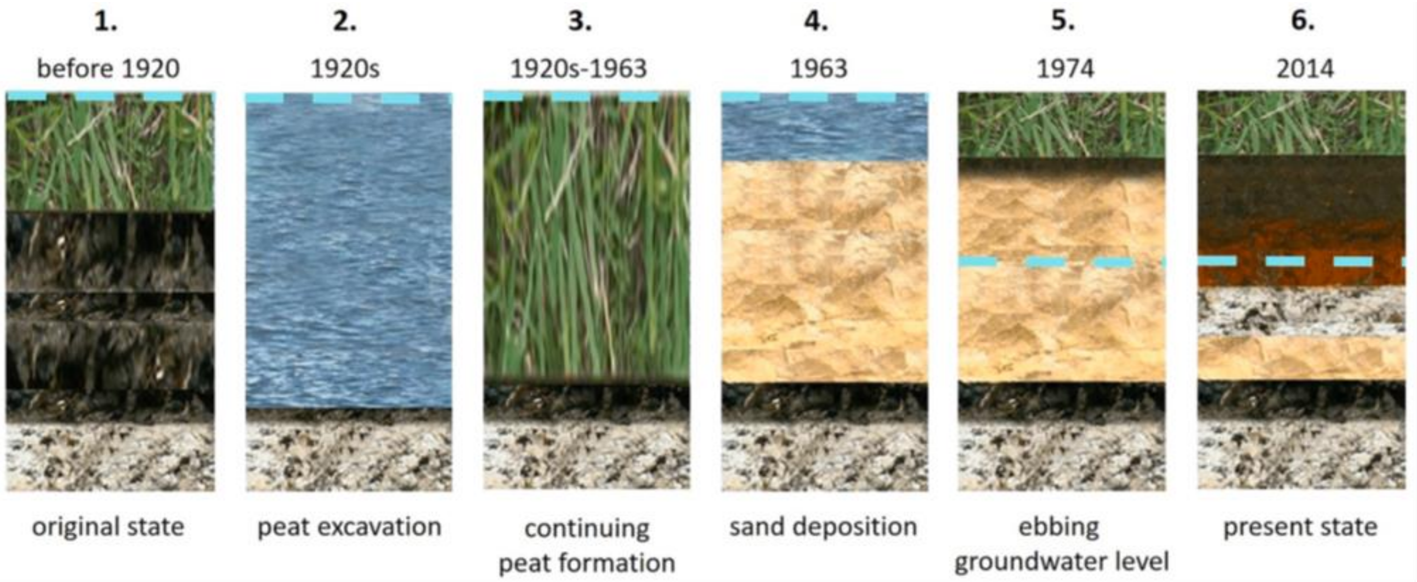

Szalai et al. 2021 GEODERMA https://doi.org/10.1016/j.geoderma.2021.115328

Sharing is encouraged SEDILAB

the study area

a histic GLEYSOL

Hec
0-10 cm

Alhc
10-20 cm

Alc
20-33 cm

Bcg
35-45 cm

Cgck
45-70 cm

Cgk
70-120 cm

2Heb
120-150 cm

SOM accumulation
(SOC ~254 g kg^{-1})
mollusc shell fragments

SOM accumulation
(SOC ~115 g kg^{-1}),
pedogenic clay minerals

(am.) Fe accumulation
(Fe_2O_3 ~450 g kg^{-1}),
pedogenic clay minerals
iron nodules with carbonates

$CaCO_3$ accumulation
($CaCO_3$ ~600 g kg^{-1})
calcretes with mixed carbonates

$CaCO_3$ accumulation
($CaCO_3$ ~170 g kg^{-1})
ferrous iron minerals

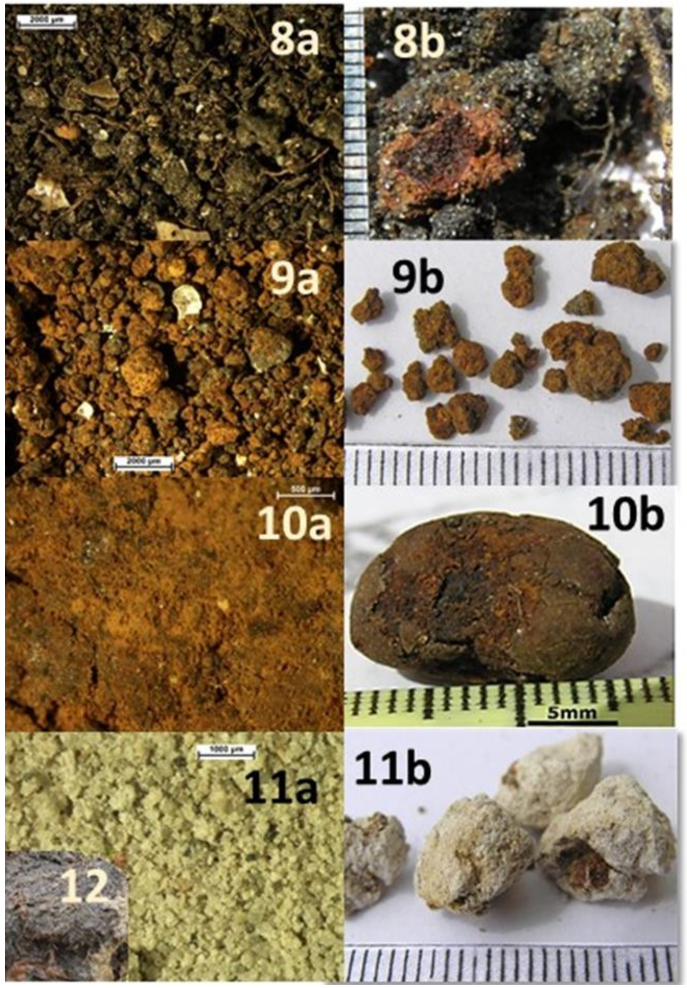

Szalai et al. 2021 GEODERMA https://doi.org/10.1016/j.geoderma.2021.115328

ever changing soil colour

Table 3. Colour of the bulk soil and its annual changes based on the Munsell colour chart

Profile	Horizon	Depth, cm	Munsell colour (moist)			
			May	August	September	October
M2	Ha	0–10	7.5YR 3/2	10YR 2/1	7.5YR 2.5/2	10YR 2/2
	Ahc	10–20	7.5YR 3/4	7.5YR 3/2	7.5YR 3/2	10YR 3/2
	Ac	20–35	7.5YR 3/4	indet.	7.5YR 4/6	10YR 2/2
			7.5YR 5/6		7.5YR 5/8	7.5YR 5/8
	Blc	35–45	7.5YR 5/6	indet.	10YR 8/2	10YR 4/1
	Ckc	45–70	10YR 7/1	10YR 7/1	10YR 7/2	10YR 8/3
	Clk	70–120	10GY 5/1	5G 7/2	5GY 6/1	10GY 5/1

Ringer et al. 2021. HGB https://doi.org/10.15201/hungeobull.70.4.6

the fluctuating redox environment (in Bcg)

Table 10

Number of alternations in iron redox state in soil horizons during three years of field monitoring (2012–2014) calculated from hourly data, and, *estimated value for 50 years.

	Gleysol M2 20 cm		Gleysol M2 40 cm		Gleysol M2 100 cm	
	2012–2014	> 50 years*	2012–2014	> 50 years*	2012–2014	> 50 years*
$Fe(OH)_3$-$Fe_3(OH)_8$ [a]	7	117	67	1117	0	0
$Fe_3(OH)_8$-$Fe(OH)_2$ [a]	0	0	11	183	0	0
Ferryhidrite-Siderite [b]	10	167	35	583	0	0
$Fe(OH)_3$-$Fe(OH)_2^c$	0	0	0	0	0	0

Redox states of the Fe minerals are calculated following (a) = Ponnamperuma et al. (1967); (b) = Meek and Chesworth (2008); and (c) = Lemos et al. (2007).

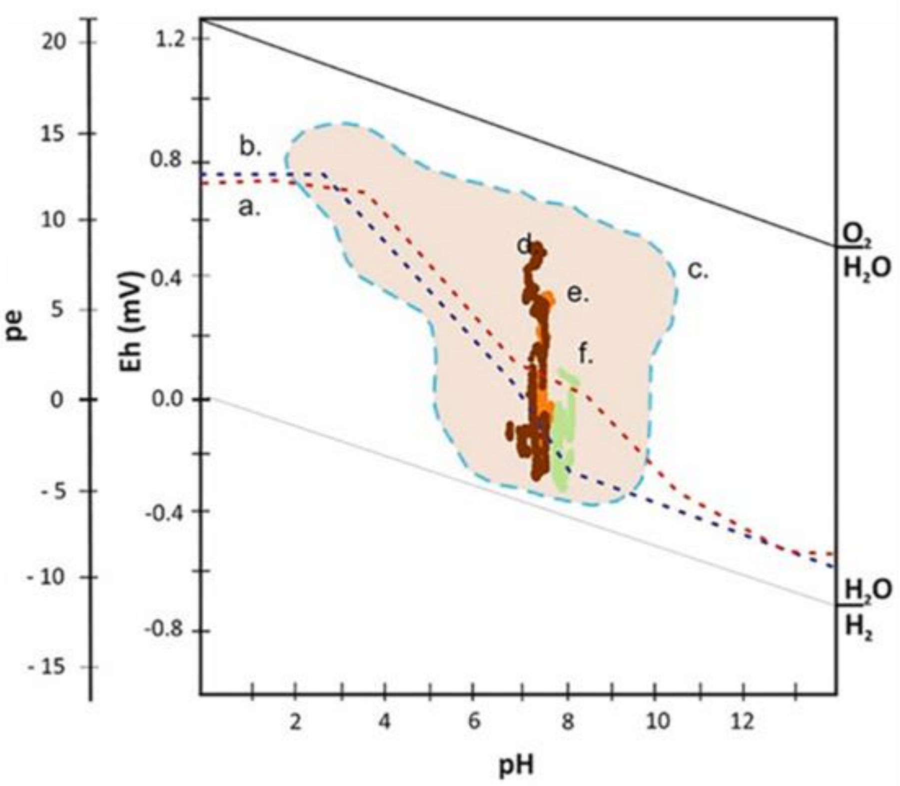

lepidocrocite

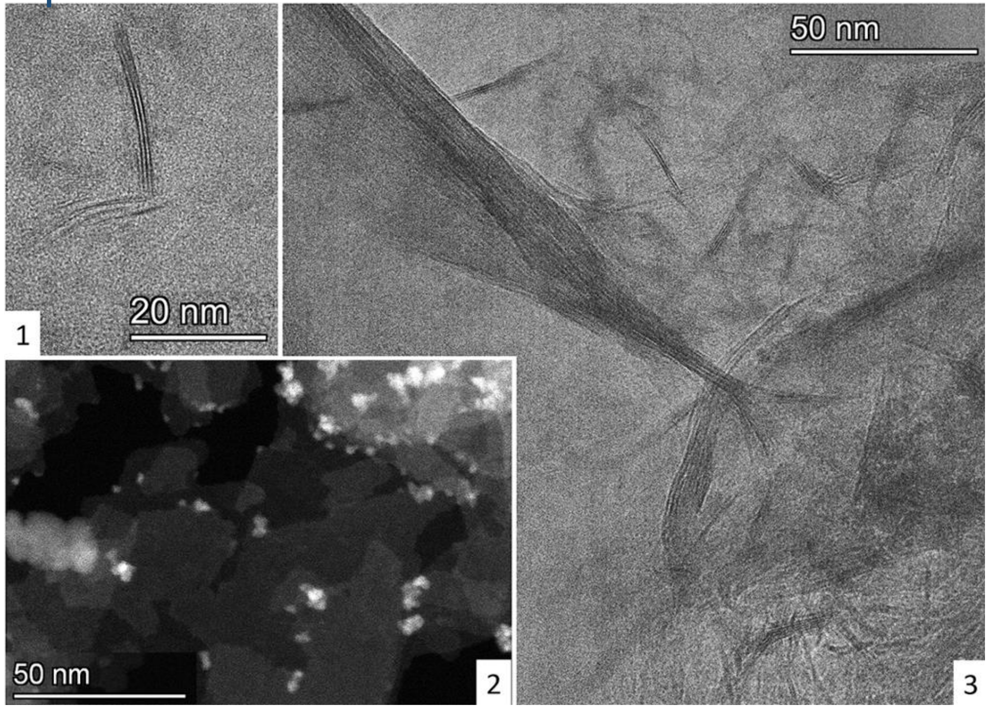

smectites

goethite on tiny smectites

Szalai et al. 2021 GEODERMA https://doi.org/10.1016/j.geoderma.2021.115328

50 yrs of profile development

Hec
0-10 cm

Alhc
10-20 cm

Alc
20-33 cm

Bcg
35-45 cm

Cgck
45-70 cm

Cgk
70-120 cm

2Heb
120-150 cm

Szalai et al. 2021 GEODERMA https://doi.org/10.1016/j.geoderma.2021.115328

1. SOM accumulation (with high POM)

2. Dissolution of mollusc shells due to slightly acidic pH
(leaching of dissolved $CaCO_3$ seasonal decline of groundwater)

3. accelerated weathering due to frequently fluctuating redox environment
- **neoformation of clay minerals**
- **neoformation of Fe3+ oxides and hydrous oxides**

4. Precipitation of $CaCO_3$ due to higher pH and mixed carbonates

Thank you for your attention!

Contents lists available at ScienceDirect

Geoderma

journal homepage: www.elsevier.com/locate/geoderma

ELSEVIER

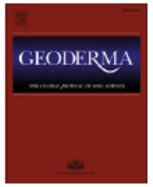

Accelerated soil development due to seasonal water-saturation under hydric conditions

https://doi.org/10.1016/j.geoderma.2021.115328

DOI: 10.15201/hungeobull.70.4.6 Hungarian Geographical Bulletin 70 2021 (4) 369–380.

Vertical differentiation of pedogenic iron forms – a key of hydromorphic soil profile development

https://doi.org/10.15201/hungeobull.70.4.6

supported by the National Research, Development, and Innovation Office (NKFIH), grant number: K-123953 and supported by the Eötvös Loránd Research Network SA41/2021